Received: 19 October 2023 | *Revised:* 17 November 2023 | *Accepted:* 20 January 2024
DOI: 10.37917/ijeee.21.2.3 *Vol. 21 | Issue 2 | December 2025*

Iraqi Journal for Electrical and Electronic Engineering
Original Article

Open Access
IJEEE University of Basrah College of Engineering

Modelling, Simulation and Control of Fuel Cell System

Mayyadah K. Salim*, Ammar A. Aldair, Osama Y. K. Al-Atbee
Electrical Engineering Department, University of Basrah, Basrah, Iraq

Correspondance
*Mayyadah K. Salim
Electrical Engineering Department
University of Basrah, Basrah, Iraq
Corresponding address
Email: pgs.mayada.kareem@uobasrah.edu.iq

Abstract
The operational variables of Proton Exchange Membrane Fuel Cell (PEMFC) such as cell temperature, hydrogen gas pressures, and oxygen gas pressures are highly effect on the power generation from the PEMFC. Therefore, the Maximum Power Point Tracker (MPPT) should be used to increase the efficiency of PEMFC at different operational variables. Unfortunately, the majority of conventional MPPT algorithms will cause PEMFC damage and power loss by producing steady-state oscillations. This paper focuses on enhancing the efficiency of the Proton Exchange Membrane Fuel Cell through the utilization of advanced control methods: Grey Wolf Optimizer (GWO), GWO with a PID controller and perturbation and observation (P&O) techniques. The objective is to effectively manage power output by pinpointing the maximum power point and reducing stable oscillations. The study evaluates these methods in swiftly changing operational scenarios and compares their performances. The obtained results show that the GWO with a PID controller increase generation power.

Keywords
Fuel Cell, PEMFC, FC Control

I. Introduction

The use of unconventional energy sources is expanding as a result of the worrisome rate of depletion and scarcity of traditional energy sources. Major conventional sources include coal, oil, gas and nuclear energy. The resources have been used continuously and have largely been depleted. Furthermore, the application of these sources make large contributions to pollution, which helps fuel global warming. The problems urge scientists to use renewable energy sources (RES). Energy sources that Non-conventional or RES are created by natural processes routinely and do not exhaust [1].

The hydrogen fuel cell, particularly the PEMFC, is one of the many renewable energy sources developing energy sources that produce clean and efficient power. It has a greater power efficiency than the process of producing regular power [2]. The Hydrogen and oxygen in a fuel cell, an electrochemically combined to create electricity, along with the byproducts of heat and water. Fuel cells offer numerous benefits over traditional power sources, primarily in terms of reduced emissions, increased efficiency, decrease noise, and quieter operation, making them an attractive alternative for various applications as society seeks cleaner and more sustainable energy options. As a result, PEMFC is an excellent choice for generating the necessary output power in a variety of applications, such as stationary power plants and automobile industry. However, in a real-world setting, operational factors such temperature, hydrogen/air partial pressure, membrane water content, stoichiometric reactant ratio, and fuel cell aging condition would have a substantial impact on the PEMFC output capacity [3].

Additionally, when PEM-FCs aged their power capacity will also decrease. The maximal PEMFC output power under changing operating conditions and PEMFC aging must thus be monitored and maintained [4]. The voltage-current characteristic for PEMFC is nonlinear, and it has a special point known as PEMFC power-current curve with MPP. The MPPT controller was proposed and implemented to PEMFC power generating system in order to guarantee that PEMFC operates

at MPP to retain maximum PEMFC output power [5]. Fuel cells create DC power, which likewise exhibits a wide range of fluctuations, and electronic power converters are crucial in converting this power [6]. It's single cell thermodynamic voltage varies between 0.8 and 1.5 V depending on the kind of fuel cell under typical working circumstances. For use Several cells are clustered together in power generation systems that demand a comparatively high amount of electricity to increase their combined power [7]. Various MPPT methods are found in literature, and these encompass techniques such as Perturb and Observe (P&O). Various algorithms like Incremental Conductance (IC), Extremum Seeking Control (ESC), Fuzzy Logic Controller (FLC), Radial Basis Function Network (RBFN), Sliding Mode Control (SMC), Particle Swarm Optimizer (PSO), Slap Swarm Algorithm (SSA), grey wolf optimizer (GWO), and ant lion optimizer are employed extensively in solar photovoltaic (PV) systems to optimize output power. Likewise, a similar method is applied to ascertain the utmost power attainable from fuel cells, capitalizing on the resemblances in power curve traits shared by both systems. A perturb and observe (P&O) method using a PEMFC was developed by Naseri et al. [8] and M.H.wang [9] to maximize the output power of a fuel cell using the MPPT method, one may compare the rate of each moment variation in power and current, the step perturbation selected to provide the most power output. This MPPT technique operates by regulating the boost converter through the control of its duty cycle, ensuring the maintenance of the fuel cell's maximum power. To increase the output power, Karami et al. [10]

tested the incremental conductance (IC) and P&O approaches for MPPT integrated using a synchronous DC-DC buck. The method using integrated circuits calculates the rate of change of fuel cell power relative to the current. Subsequently, maximum power can be found at the point where the derivative result equals zero. IC required less time tracking when compared to the P&O approach. It was more steady exogenous variations of the components existed Fuzzy logic control (FLC) and particle swarm optimizer (PSO)-based MPPT for fuel cell stacks were introduced and contrasted by Luta and Raji [11] by using methods PSO and FLC-based MPPT that regulate the DC-DC boost controller fuel cell power at its highest level. Jiao and Cui [12], as well as Afshar et al. [13], introduced a MPPT system for a fuel cell power setup that employs sliding mode control (SMC) combined with a DC-DC boost converter. The function of sliding mechanism adjusts the output control for the duty cycle. The findings indicate that the SMC method preserved the highest output power of the fuel cell, and it could withstand a range of external forces conditions. The PSO-based MPPT was enhanced by Ahmadi et al. [5] utilizing a proportional-integral-derivative (PID) controller. P&O and SMC appro-aches are then used to compare

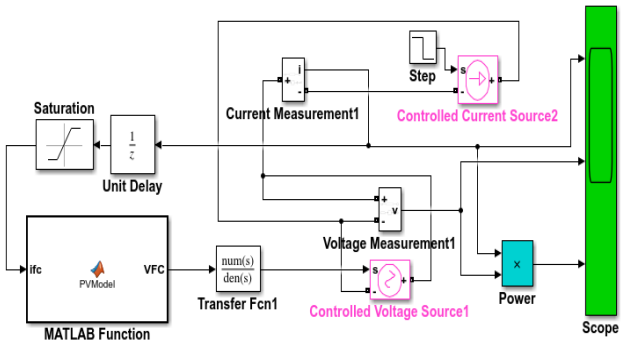

Fig. 1. The Simulink model of a PEMFC system

the outcomes. The PSO-PID technique simulation had the best results because it tracked the maximum power point in varying conditions with great precision, quick time reaction, and extremely little power fluctuation. An extreme seeking control (ESC) for MPPT with a DC-DC boost converter in a PEMFC system was presented by Derbeli et al. [14]. The ESC monitors the fuel cell MPP when it is in use. The study included both simulated and experimental data. The results suggest that extremum-seeking control proved to be a successful method for monitoring the Maximum Power Point (MPP) of the fuel cell. There was however 9% to 10% power fluctuation in the in the power output from the fuel cell. The oscillation may cause PEMFC damage, power loss, and decreased operational efficiency. Recent studies concentrate on intelligent optimization methods with great precision and efficiency, which can eliminate the power fluctuation around the MPP brought on by the conventional technique. In this paper, an MPPT strategy based on a GWO-PID controller is presented for PEMFC systems operating at various temperatures, hydrogen gas pressures, and oxygen gas pressures. The suggested technique for determining the fuel cell ideal operating voltage system and modifies the fuel cell system operating point to the maximum power by adjusting the duty cycle of the boost converter.

II. Fuel Cell System Modelling

A PEMFC stack, MPPT controller, and a DC/DC boost converter are all components of a comprehensive PEMFC power production system. It is imperative to investigate the mathematical modeling and attributes of PEMFC systems. The power output characteristics of the fuel cell exhibit nonlinearity and are influenced by variables such as cell temperature, oxygen partial pressure, hydrogen partial pressure, and membrane water content [5]. The Simulink model with matlab of a PEMFC system shown in Fig. 1.

Sir William Grove developed fuel cells, which are now a practical energy source. In its most basic form, fuel cells

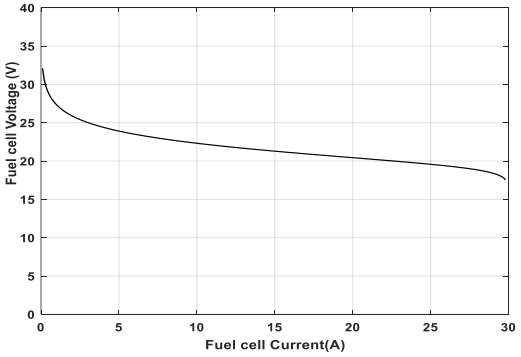

Fig. 2. PEMFC V-I polarization curve

may be compared to generators. Fuel cells generate electricity without relying on moving components, unlike conventional generators that utilize internal combustion engines to power an alternator. Fuel cells quite reliable and effective as a consequence. It is acceptable for use indoors. Fuel cells display complex and nonlinear voltage-current characteristics. As shown in Fig. 2. a polarization curve illustrates the complex relationship between the current and voltage of a fuel cell. The voltage produced by the fuel cell is regulated by the current, a factor influenced by various operational parameters.

Eq. 1 is the formula specifying the voltage produced by the fuel cell [15].

$$V_{\text{cell}} = E_{\text{Nernst}} - V_{\text{act}} - V_{\text{ohm}} - V_{\text{conc}} \tag{1}$$

where E_{Nernst} is a thermodynamic potential that can reverse, as indicated by Nernst Eq. 2.

$$\begin{aligned} E_{\text{Nernst}} &= 1.229 - 0.85 \times 10^{-3}(T - 298.15) + \\ &\quad 4.31 \times 10^{-5} T \left(\ln P_{H_2} + 0.5 \ln P_{O_2}\right) \end{aligned} \tag{2}$$

where T stands for the absolute temperature in kelvins, P_{H_2} represents hydrogen partial pressure, and $P_{O_2}$the partial pressure of oxygen. V_act is the activation voltage drop provided by Eq. 3 .

$$V_{\text{act}} = -\left(\zeta_1 + \zeta_2 T + \zeta_3 T \ln\left(C_{O_2}\right) + \zeta_4 T \ln\left(I_{FC}\right)\right) \tag{3}$$

here, the dissolved-oxygen content in the interface of the cathode catalyst is denoted by C_{O_2}, where $\zeta_i (i = 1-4)$are parametric coefficients for each cell model. and $\zeta_i = 1, ..., 4$ which are parametric coefficients for each cell model. This information is found in Eq. 4.

$$C_{O_2} = \frac{P_{o_2}}{(5.08 \times 10^6) \times \exp(-498/T)} \tag{4}$$

Using Eq. 5, the entire ohmic voltage drop is computed.

$$V_{\text{ohm}} = I_{FC}\left(R_M + R_c\right) \tag{5}$$

R_M denotes the ohmic resistance, encompassing the resistance from both the electrodes and the polymer membrane, along with the resistance inherent in the electrodes themselves. R_c considered constant value represents the resistance encountered by protons as they traverse the membrane. The Eq. 6 provides R_M in this case.

$$R_M = \frac{r_m t_m}{A} \tag{6}$$

where t_m ,represents the thickness of the membrane in centimeters, A denotes the activation area in square centimeters, and r_m signifies the membrane resistivity in ohm-centimeters related to proton conductivity. The resistivity of the membrane is notably influenced by both membrane humidity and temperature, and this relationship is mathematically expressed as Eq. 7 [16].

$$r_m = \frac{181.6\left[1 + 0.03\left(I_{FC}/A\right) + 0.062(T/303)^2\left(I_{FC}/A\right)^{2.5} J\right.}{\left[\lambda_m - 0.634 - 3\left(I_{FC}/A\right)\right] \times exp(4.18(T - 303/T))} \tag{7}$$

where the λ_m represents the membrane water content and serves as a PEMFC model input. It also depends on the average water activity a_m, which is described by Eq. 8.

$$\lambda_m = \begin{cases} 0.043 + 17.81 a_m - 39.85 a_m^2 + 36 a_m^3, 0 < a_m < 1 \\ 14 + 1.4\left(a_m - 1\right), \quad 1 < a_m \leq 3 \end{cases} \tag{8}$$

Eq. 9 describes the connection between the average water activity and the water vapor partial pressures at the anode and cathode, respectively.

$$a_m = \frac{1}{2}\left(a_{an} + a_{ca}\right) = \frac{1}{2}\frac{P_{v,an} + P_{v,ca}}{P_{sat}} \tag{9}$$

Eq. 10 empirical formulation can be used to compute the saturation pressure of water P_{sat}. [17]

$$\log_{10} P_{\text{sat}} = -2.1794 + 0.02953T - 9.1813 \times 10^{-5} T^2 + 1.4454 \times 10^{-7} T^3 \tag{10}$$

The range of λ_m values is 0 to 23. The reduction in concentration voltage is put into Eq. 11

$$V_{\text{conc}} = -B \ln\left(1 - \frac{J}{J_{max}}\right) \tag{11}$$

Where B expresses the regulating parametric coefficient. J and J_max are the current density and the maximum current density ($A\ cm^{-2}$). To generate the desired voltage, fuel cells are connected in a series arrangement $N_F C$. This leads to the individual $N_F C$ cells within each string displaying nonlinear voltage-current (V-I) characteristics, as specified in the Eq. 12. In conclusion, the process of determining the fuel cell output voltage involves combining the equations provided earlier. It is important to note that the voltage generated by an individual cell is quite limited. Consequently, the solution is to connect numerous cells to a bipolar plate to boost the output voltage. As a result, the output voltage of the PEMFC is directly correlated with the number of cells N. This relationship is expressed through the equation defining the output power (W) of the PEMFC. According to Eq. 12, series cells inside a string exhibit nonlinear VI properties.

$$V_{FC} = N_{FC} V_{\text{cell}} \tag{12}$$

The specified formula for the power output (in watts) of a Proton Exchange Membrane Fuel Cell (PEMFC) can be described as follows:

$$P_{FC} = V_{FC} I_{FC} \tag{13}$$

The intended system is implemented in MATLAB /Simulink to test the effectiveness of the proposed MPPT approach. The MPPT method is provided in the next section after the PEMFC model and boost converter.

III. DC/DC Boost Converter

Power converters are electronic devices widely applied in industry, and in recent years, for renewable energy electronic systems, boost converter can regulate voltage levels to a higher level [18].

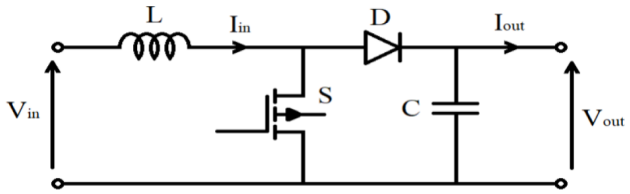

Fig. 3. DC-DC boost converter

TABLE I.
THE SPECIFICATIONS OF THE DESIGNED CONVERTER

Description	Parameter	Nominal value
Input voltage	V_{IN}	20V
Capacitance	C	0.0668F
Inductance	L	0.0354H
Switching frequency	f_s	5000HZ
Desired output voltage	V_{OUT}	48V

In a PEMFC power production system, the DC/DC boost converter is employed as a link between the PEMFC and the load. By adjusting a duty cycle to conform to the PEMFC MPP, the converter may vary the cell operating current and raise the PEMFC output voltage. A capacitor C, an inductor L, a diode D, and a switch make up a full DC/DC boost converter [19]. Obtaining the necessary materials is crucial for maintaining a consistent production. The specifications of the designed converter are given in Table I.

IV. MPPT Technique

The MPPT algorithm is employed to achieve the highest possible power output from an energy source. MPPT management is essential for a PEMFC power system to operate efficiently. According to the PEMFC math-ematical modeling, tweaks to its parameters can have a big impact on how much power the fuel cell produces. The primary issue tackled by the MPPT is that the efficiency of the PEMFC is contingent on the supplied Partial Pressure of Reactant Gases and Cell temperature. To maintain optimal efficiency, the system needs optimize to reach the level that aligns closest to the point where the PEMFC generates its highest available power. Consequently, the primary goal of the MPPT is to identify the Maximal Power Point (MPP) and compel the PEMFC to function at that precise point. These techniques aim to determine the voltage or current at which the fuel cell system provides its highest power output. This approach assists in surmounting the challenges associated with selecting the most efficient voltage, especially when influenced by variations in input parame-

ters. In this section, we introduce MPPT method based on Grey Wolf Optimization and Proportional-Integral-Derivative (GWO-PID). Additionally, we delve Grey Wolf Optimizer (GWO) and perturbation and observation (P&O) for comparison with our proposed algorithm. These algorithms will be described in the following subsections. The MPPT technique was developed and implemented in the PEMFC system, where it collaborates with the DC-DC boost converter. This MPPT algorithm is responsible for managing the boost converter switch and ensuring the fuel cell output voltage is at its Maximum power level. When the PEMFC is linked to the DC-DC boost converter, the fuel cell output voltage serves as the input voltage for the boost converter. After the MPPT algorithm determines the switch status, it transmits a signal to command the boost converter switch. As a result, the switch will either turn on or off based on the instructions provided by the MPPT controller. In the end the boost converter maintains the fuel cell output voltage at its maximum power level.

A. Greywolf Optimization Algorithm

The GWO, introduced in [20], finds its inspiration in the social dynamics of grey wolves, which typically thrive in groups ranging from 5 to 12 individuals. To replicate the leadership structure within the GWO algorithm, it incorporates four distinct levels: $\alpha, \beta, \delta and \omega$. Alpha, serving as the male and female leaders of a pack, assumes the primary responsibility for crucial decisions, such as hunting and determining sleep and wake-up times. Beta's role involves assisting alpha in decision-making and providing feedback and suggestions. Delta undertakes various responsibilities such as the scouting, sentinel duty, caretaking, elder guidance, and hunting. They oversee the omega wolves by obeying the directives issued by alpha and beta. The omega wolves, reciprocally, are bound to follow the instructions from all other wolves. Within the GWO structure, α, β, δ take charge of the hunting procedure, with the ω wolves trailing behind them in their guidance. The GWO's encircling behavior is calculated based on the structured hierarchy and interactions existing within these hierarchical levels. Fig. 4 depicts the flowchart outlining the GWO optimization method. The mathematical formulas that dictate the GWO algorithm can be summarized in the following manner:

$$\vec{X}(t+1) = \vec{X}_P(t) - \vec{A} \cdot \vec{D} \tag{14}$$

where $\vec{A}, \vec{D}$are coefficient vectors, $\vec{X}_P(t)$ is the prey's positions vector, $\vec{X}$ mimics the position vectors of wolves, (t) is the iterations number, and$\vec{D}$ is denoted as follows:

$$\vec{D} = \left| \vec{C} \cdot \vec{X}_P(t) - \vec{X}(t) \right| \tag{15}$$

where $\vec{A}, \vec{C}$are donated as following:

$$\vec{A} = 2\vec{a} \cdot \vec{r}_1 - \vec{a} \tag{16}$$

$$\vec{C} = 2 \cdot \vec{r}_2 \tag{17}$$

The vectors $\vec{r}_1, \vec{r}_2$ are randomly distributed within the range of [0, 1]. The vector $\vec{a}$ linearly decreases from 2 to 0 across iterations. Within the hunting behavior of grey wolves, the alpha is identified as the prime candidate for the solution, while beta and delta are assumed to possess some knowledge about the potential location of the prey. Consequently, the three best solutions encountered up to a particular iteration are retained, and this compels others (e.g., omega) to adjust their positions in the decision space towards the optimal locations determined by the best solutions.Where $\vec{X}_1, \vec{X}_2$ *and* $\vec{X}_3$ are defined and calculated as following:

$$\begin{gathered} \vec{X}_1 = \vec{X}_\alpha - \vec{A}_1 \cdot \left(\vec{D}_\alpha \right), \vec{X}_2 = \vec{X}_\beta - \vec{A}_2 \cdot \left(\vec{D}_\beta \right), \\ \vec{X}_3 = \vec{X}_\delta - \vec{A}_3 \cdot \left(\vec{D}_\delta \right) \end{gathered} \tag{18}$$

The updating positions mechanism can be calculated as follows:

$$\vec{X}(t+1) = \frac{\vec{x}_1 + \vec{X}_2 + \vec{X}_3}{3} \tag{19}$$

Where $\vec{X}_1, \vec{X}_2$ *and* $\vec{X}_3$ are the three best wolves (solutions) in the swarm at a given iteration t. Where $\vec{A}_1, \vec{A}_2$ *and* $\vec{A}_3$ are calculated as in Eq (18). $\vec{D}_\alpha, \vec{D}_\beta$ *and* $\vec{D}_\delta$ are calculated as in Eq. 20.

$$\begin{gathered} \vec{D}_\alpha = \left| \vec{C}_1 \cdot \vec{X}_\alpha - \vec{X} \right|, \vec{D}_\beta = \left| \vec{C}_2 \cdot \vec{X}_\beta - \vec{X} \right|, \\ \vec{D}_\delta = \left| \vec{C}_3 \cdot \vec{X}_\delta - \vec{X} \right| \end{gathered} \tag{20}$$

The values of $\vec{C}_1, \vec{C}_2$ *and* $\vec{C}_3$ are computed according to Eq. 17. In the GWO algorithm, a critical element for adjusting the balance between exploration and exploitation is the vector $\vec{a}$ The algorithm's primary documentation proposes a linear decrease in this vector across each dimension, proportionate to the number of iterations, from an initial value of 2 down to 0. The equation used for updating it is as follows:

$$\vec{a} = 2 - t \cdot \frac{2}{t_{max}} \tag{21}$$

where t is the iteration number, ter is the optimization total iterations number.

B. GWO with PID Technique Problem Formulation

The effectiveness of a system is measured using a performance index. The performance of a PID controller is commonly depicted through such an index, aiding in the design of systems that meet the desired parameters effectively. Eq. 22 provides the integral of the absolute error (IAE) performance index which is the most common performance metrics among control system engineers :

$$IAE = \int_0^\infty |e(t)|dt \tag{22}$$

For assessing and enhancing the performance of systems, processes, or models, performance indices and error calculations are crucial tools. While error computations provide precise information about the correctness and dependability of results, performance indices provide a high level assessment of overall performance. Both are essential for producing well-informed judgments and optimizations. The actual result might either overestimate or underestimate the predicted value, and the error is often stated as a numerical value with a positive or negative sign. The system's ability to perform and achieve its intended outcomes is evaluated based on the degree of discrepancy or inaccuracy present.

C. The Procedures GWO With PID Technique

Utilizing the GWO technique, the following procedures can be used to optimize the PID controller settings for a proton exchange membrane fuel cells:

1. Clearly state the issue: To start, you must define the issue and specify the variables that must be under control. Here, the goal is to manage the fuel cell's output power by optimizing the PID controller's settings.
2. Establish the GWO algorithm. The population size, maximum number of iterations, and search range for each parameter must all be specified for the GWO algorithm. The PID controller settings for the PEMFC may be optimized using the GWO technique.
3. Describe the goal function: The PID controller effectiveness is assessed using the fitness function. In this scenario, the controller ability to control the fuel cell's output power should be measured by the fitness function.
4. Select a PI controller: In control systems, a proportional-integral (PI) controller is frequently used to govern a process variable. It is a kind of feedback controller that modifies the control signal based on the difference between the desired setpoint and the measured process variable.
5. Establish the controller parameters: The proportionate gain (Kp) and integrating gain (Ki) of the PI controller need to be modified. These variables affect the controller responsiveness and may be changed to enhance the fuel cell output power.

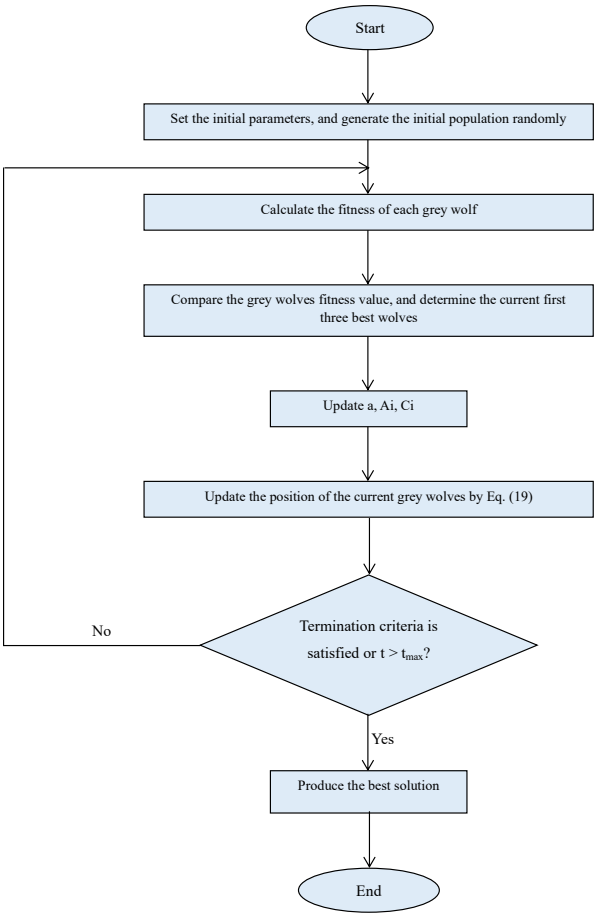

Fig. 4. The flow diagram of the GWO-based MPPT method.

6 . Utilize the Grey Wolf Optimization (GWO) algorithm: This population-based optimization method draws inspiration from the hunting strategies observed in grey wolves. It is a metaheuristic optimization algorithm that may be employed to identify the best answers to challenging issues. The PI controller settings for a proton exchange membrane fuel cell may be optimized using GWO.
7. Execute the optimization: After the GWO method has been set up, it can be utilized to determine the ideal Kp and Ki values for the PI controller. Up until the fitness function is optimized, the GWO algorithm will iteratively cycle over the population and change the values of Kp and Ki.
8. Examine the results.

D. Perturb and Observe–Based MPPT

Most authors and practitioners commonly utilize the 'P&O' method as a primary approach for achieving the Maximum Power Point (MPP). The P&O algorithm relies on introducing a disturbance to the voltage of the fuel cell. This dis-

turbance, positive or negative determined by the preceding power value [21]. This method aims to maintain proximity to the MPP. The fundamental process is outlined in Fig. 5 flowchart. As per this diagram, if the FC system power increases, the alteration in the reference voltage remains in the same direction to reach the MPP. Conversely, if there is a decrease in FC output power, the disturbance polarity changes. The P&O technique is widely used due to its simplicity and straightforward application. Nevertheless, it has limitations under rapidly changing operating conditions [22]. Additionally, it exhibits oscillations around the MPP, particularly with larger disturbance step-sizes, and it possesses a relatively slow response time due to the fixed step-size applied.

V. Simulation Results

The various operational parameter settings will be used to examine the parametric influence on the fuel cell power. six experiments were taken into consideration, including normal operating conditions, variation operating conditions of the temperature, variation operating conditions of hydrogen gas pressure and oxygen gas pressure. To validate the precision and effectiveness of the GWO-PID MPPT controller, a comparison was conducted against both P&O and GWO without PID. Subsequently, the discussion presents the values of relevant parameters observed across different scenarios. To evaluate the efficacy of the suggested MPPT method, MATLAB /Simulink is employed to execute the designed system. The Simulink model of the MPPT system for PEMFC illustrated in Fig. 6. MPP tracker connects the fuel cell system to the battery. The MPP tracker contains the boost dc-dc converter, GWO-MPPT and PID controller. The boost converter circuit comprises of diode, capacitor C, IGBT switch and inductor L. A Lead-Acid battery with rated at 48 V, 200 Ah is used for the power storage. Using a battery as a load provides advantages in terms of energy storage and dynamic load simulation. However, various operational conditions such as load fluctuations, system efficiency, and battery characteristics can significantly impact the charging of the battery in an MPP tracker system for fuel cells. Optimizing the system design and control algorithms becomes crucial to ensure efficient energy utilization and effective battery charging under diverse conditions.

A. Case1: Constant Operational Condition

In this instance, the temperature (T) has been set to 333K ,the membrane water content (λ) is 23, hydrogen gas pressure is 1 atm and oxygen gas pressure is 0. 2095. The GWO/PID, GWO, and P&O may all maneuver about the MPP as shown in Fig. 7. It clear that P&O will be the cause of the power fluctuations around the MPP. The GWO-PID and GWO methods successfully extract the (MPP) in contrast to the conventional method, resulting in stable output power during the steady

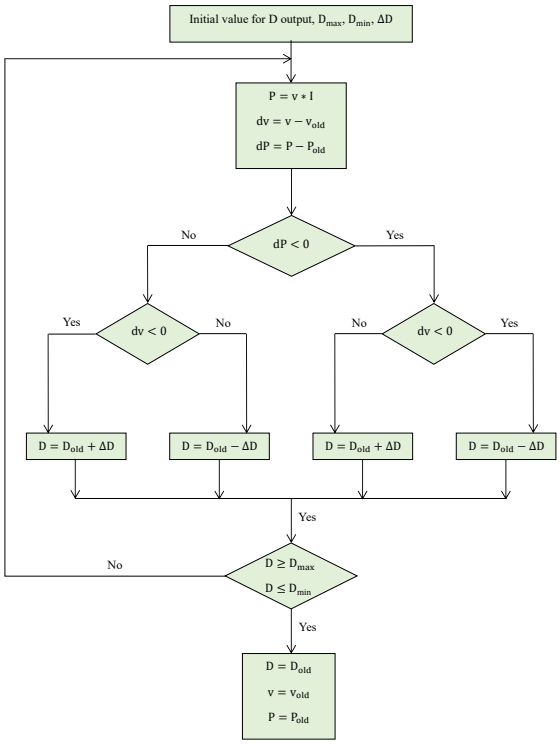

Fig. 5. The flow diagram of the P&O-based MPPT method.

state. Additionally, GWO-PID has a tracking speed that is quicker than GWO. the algorithm recurrent search for the MPP reveals that the GWO-PID has less amplitude fluctuations than the GWO. It performs better than regular GWO because of its quickness and minimal amplitude fluctuations. The total error displays how precisely, dependably, and successfully the system operates. For a system to function better and produce required results, mistakes must be managed and reduced especially in applications where accuracy and consistency are vital, as shown in Fig. 8. It clear that GWO-PID is the best.

B. Case 2: Variation Operating Condition of the Temperature

The MPPT control system is run under fast fluctuations in temperature T with being water content of the membrane, hydrogen gas pressure, oxygen gas pressure taken into account as a constant value equal to 23,1 with the goal of assessing the dynamic tracking capabilities of the GWO-PID algorithm while operating circumstances vary. Initially 303K is chosen as the temperature. After 4 seconds the temperature is raised to 333K, after 8 seconds temperature is raised to 363K. In Fig. 9. Both GWO-PID and GWO have superior accuracy and stability as compared to conventional P&O. When searching

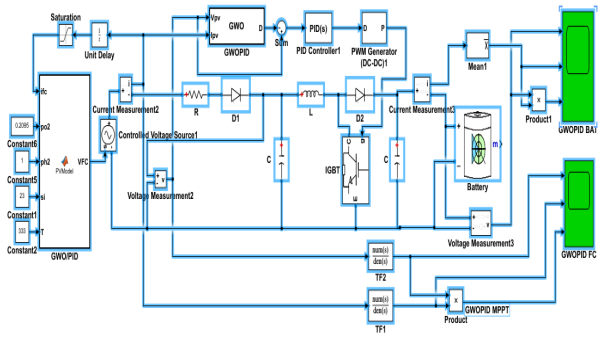

Fig. 6. GWO-PID MPPT Configuration.

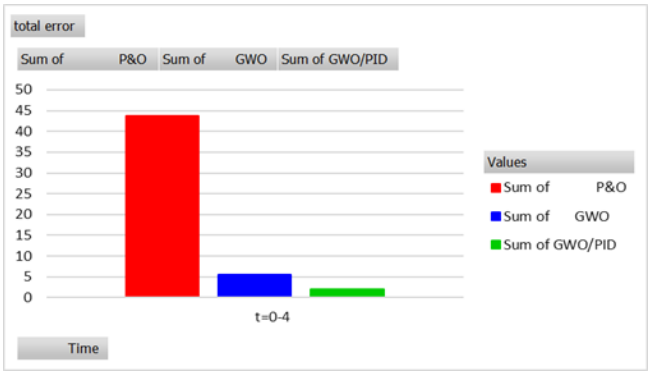

Fig. 8. Total error of MPPT under constant operational condition.

the MPP, GWO-PID performs better than GWO as higher tracking speed and less amplitude oscillation. Employing the P&O algorithm for MPPT and optimizing the control parameters using GWO or GWO-PID can contribute to minimizing errors in a fuel cell system. P&O adjusts the operating point to track the maximum power, while GWO and GWO-PID optimize control parameters to enhance the overall system performance and reduce errors. as shown in Fig. 10. It clear that GWO-PID is the best.

C. Case 3: Variation Operating Condition of the Hydrogen Gas Pressure

Another crucial element that influences the PEMFC's ability to generate electricity is the hydrogen gas pressure. while T is fixed at 333K. First, the hydrogen gas pressure 0.4, It increases to 1 after 4 seconds. It is once more increases to 1.6 at 8 seconds Fig. 11 demonstrates the differences between various methods as well as the dynamic response to varying hydrogen gas pressure. The P&O approach, which creates oscillation around the MPP provides a bigger power loss and may harm the fuel cell, according to this statistic. The GWO-PID also exhibits less amplitude oscillations than GWO. Additionally, GWO-PID has a higher convergence speed and less amplitude oscillation throughout the search process than GWO. Increase the pressure of hydrogen gas supplied to the fuel cell led to increased power output from the fuel cell. The GWO-PID algorithm reduces the total error in fuel cell power by leveraging the GWO optimization process to fine-tune the parameters of a PID controller. This integration enhances the control system ability to regulate the fuel cell power output, resulting in improved performance and minimized errors. as shown in Fig. 12. It clear that GWO-PID is the best.

D. Case 4: Variation Operating Condition of the Oxygen Gas Pressure

The pressure of oxygen gas can have a significant effect on the output power and overall performance of the fuel cell.

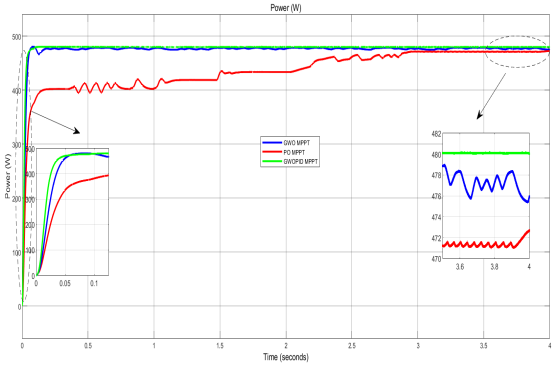

Fig. 7. MPPT under constant operational condition.

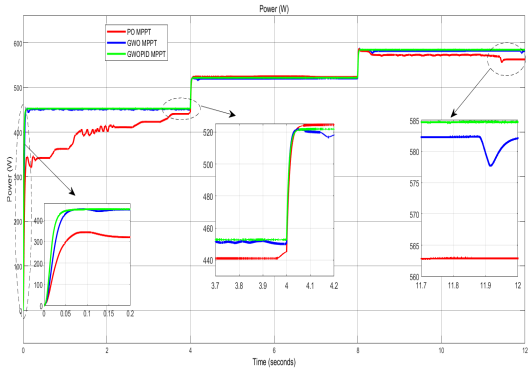

Fig. 9. MPPT under Variation operating condition of the temperature.

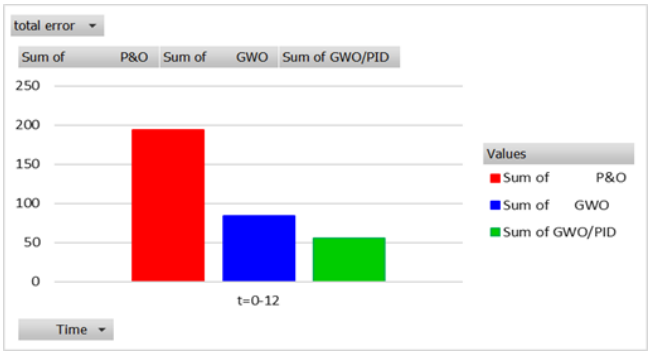

Fig. 10. Total error of MPPT under Variation operating condition of the temperature.

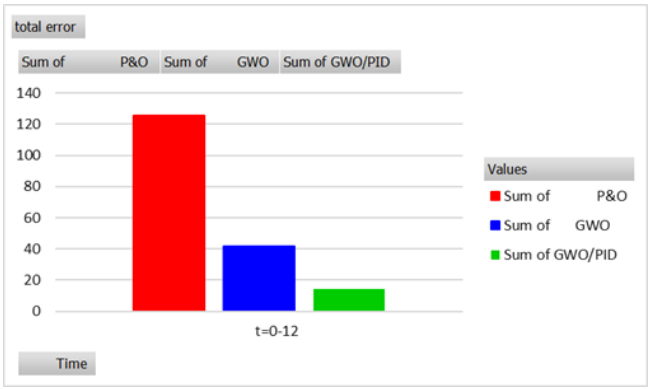

Fig. 12. Total error of MPPT under Variation operating condition of the hydrogen gas pressure.

First, the oxygen gas pressure 0.1095, at time=4s it increases to 0.2095. It is once more increases to 0.3095 at 8 seconds. Higher oxygen pressure provides more reactant molecules at the cathode, increasing the rate of electrochemical reactions. This effect generally result in increased power output. seen in Fig. 13. as compared to conventional P&O, both GWO/PID and GWO have superior accuracy and stability. When searching the MPP, GWO/PID performs better than GWO as higher tracking speed and less amplitude oscillation. In a fuel cell system, ”total error” refers to the cumulative errors, inaccuracies, or deviations that occur during the operation or control of the system a variety of factors can lead to these errors, such as fluctuations in operating conditions, or limitations in the control algorithms used to regulate the system. Managing and reducing total error is crucial for ensuring the reliable and efficient performance of the fuel cell system. as shown in Fig. 14.It clear that GWO-PID is the best.

E. Case 5: Variation Operating Condition of the Hydrogen and Oxygen Gas Pressure

The pressure of hydrogen gas starts at 0.4 and rises to 1 after 4 seconds, then further increases to 1.6 at 8 seconds. In the case of oxygen gas, it begins at 0.1095, elevates to 0.2095 at 4 seconds, and again increases to 0.3095 at 8 seconds. Fig. 15 demonstrates the differences between various methods as well as the dynamic response to varying hydrogen and oxygen gases pressure. The P&O approach, which creates oscillation around the MPP provides a bigger power loss and may harm the fuel cell, according to this statistic. The GWO-PID also exhibits less amplitude oscillations than GWO. Additionally, GWO-PID has a higher convergence speed and less amplitude oscillation throughout the search process than GWO. Increase the pressure of hydrogen and oxygen gases supplied to the fuel cell led to increased power output from the fuel cell. The GWO-PID algorithm reduces errors in a control system by integrating the GWO optimization algorithm with a PID

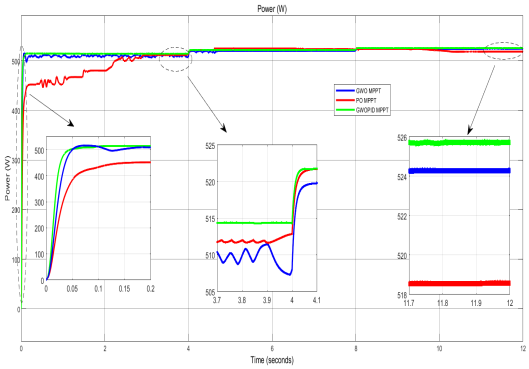

Fig. 11. MPPT under Variation operating condition of the hydrogen gas pressure.

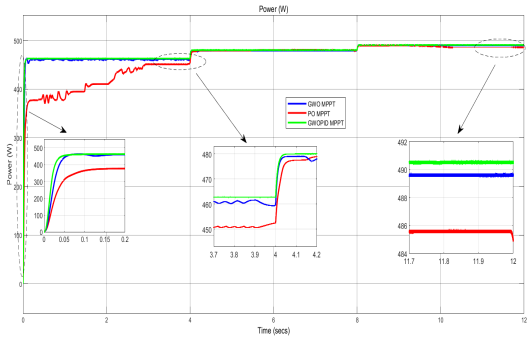

Fig. 13. MPPT under Variation operating condition of the oxygen gas pressure.

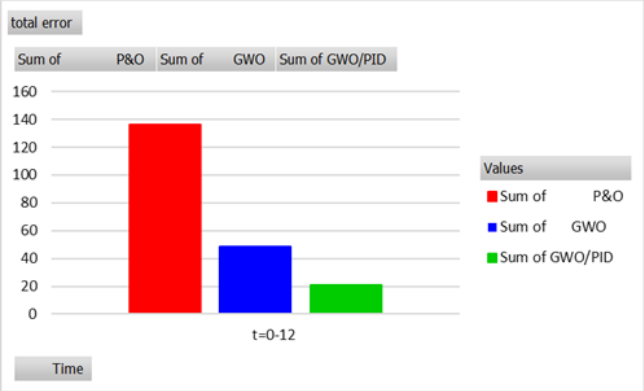

Fig. 14. Total error of MPPT under Variation operating condition of the oxygen gas pressure.

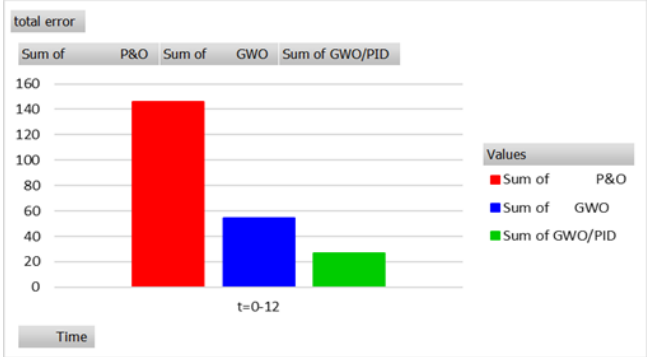

Fig. 16. Total error of MPPT under Variation operating condition of the hydrogen and oxygen gas pressure.

controller. This integration optimizes the PID parameters leading to improved adaptability and reduced discrepancies between the desired and actual system responses. As shown in Fig. 16. It clear that GWO-PID is the best.

F. Case 6: Variation Operating Condition of the Temperature, Hydrogen and Oxygen Gases Pressure

Temperature, Hydrogen pressure, and the pressure of the oxygen gas all have an impact on PEM fuel cell efficiency. The fuel cell voltage and current output increase with increasing oxygen gas pressure, hydrogen gas pressure, and temperature values. 303K is the initial temperature setting. After 4 seconds, the temperature goes up to 333K. The temperature gets higher to 363K after 8 seconds, and the hydrogen gas pressure is 0.4. After 4 seconds, it climbs to 1 and 1.6 at time=8s respectively. The oxygen gas pressure 0.3095 then at time=4s, lowers to 0.2095 as it decreased to 0.1095 at time=8s.As can be observed in Fig. 17, The GWO-PID combination demonstrates superior performance when compared to GWO and P&O methods. P&O exhibits sluggish time response and significant power fluctuations around the (MPP). On the other hand, GWO exhibits reduced power fluctuations and improved time response compared to P&O while tracking the MPP. The GWO-PID algorithm achieves a comprehensive reduction in errors by merging the GWO optimization process with a PID controller. This integration optimizes the PID parameters, enhancing system adaptability for improved regulation and minimized errors over time, as depicted in Fig. 18 It is evident that GWO-PID stands out as the most effective approach

VI. Conclusion

The operating conditions significantly affect the PEMFC characteristic curve. The MPP varies according to different operating conditions. The goal of this study is to boost the PEMFCs power capacity by introducing an MPPT controller based on GWO with PID to track the MPP. To evaluate the performance of a recommended MPPT controller, an MPPT system is built

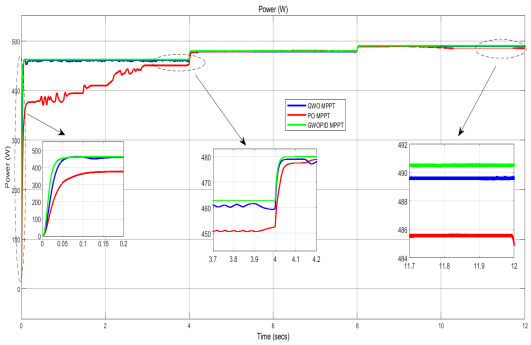

Fig. 15. MPPT under Variation operating condition of the hydrogen and oxygen gas pressure.

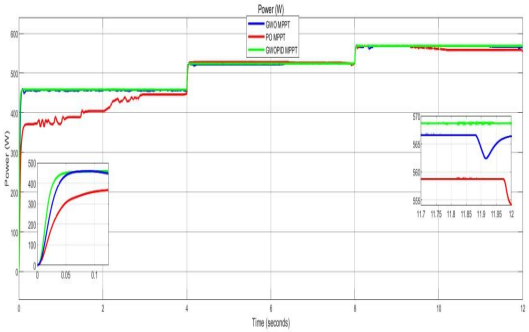

Fig. 17. MPPT under Variation operating condition of the Temperature, hydrogen and oxygen gases pressure.

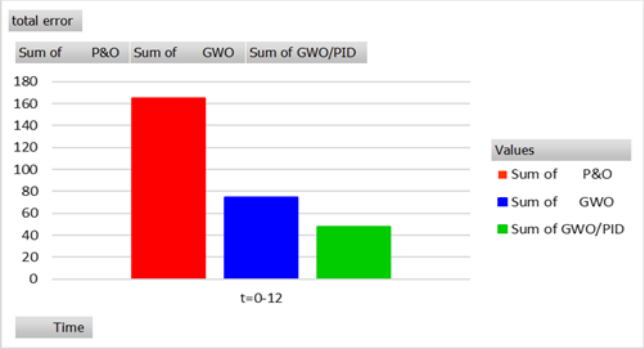

Fig. 18. Total error of MPPT under Variation operating condition of the Temperature, hydrogen and oxygen gases pressure.

in MATLAB/Simulink. The GWO/PID, which has fewer parameters and can alter inertia weight, is detailed for MPPT in this paper. To validate the performance of the GWO/PID, six scenarios are employed, including fixed operating conditions and changing operating conditions for temperature and gas pressure. The results achieved when comparing the GWO/PID with GWO and P&O show that the GWO/PID not only performs better than P&O in terms of tracking speed and amplitude oscillation, Moreover, GWO-PID exhibits a faster tracking speed and generates smaller amplitude oscillations during the optimization process compared to GWO. This method is therefore able to handle changes that may occur in the PEMFC. when compared with GWO and P&O, the GWO-PID algorithm more effective in optimizing PID parameters for reducing errors in fuel cell output power.

Conflict of Interest

The authors have no conflict of relevant interest to this article.

References

[1] B. K. Bose, "Global warming: Energy, environmental pollution, and the impact of power electronics," *IEEE Industrial Electronics Magazine*, vol. 4, no. 1, pp. 6–17, 2010.

[2] V. Boscaino, R. Miceli, and G. Capponi, "Matlab-based simulator of a 5 kw fuel cell for power electronics design," *International Journal of Hydrogen Energy*, vol. 38, no. 19, pp. 7924–7934, 2013.

[3] Z.-d. Zhong, H.-b. Huo, X.-j. Zhu, G.-y. Cao, and Y. Ren, "Adaptive maximum power point tracking control of fuel cell power plants," *Journal of Power Sources*, vol. 176, no. 1, pp. 259–269, 2008.

[4] P.-Y. Chen, K.-N. Yu, H.-T. Yau, J.-T. Li, and C.-K. Liao, "A novel variable step size fractional order incremental conductance algorithm to maximize power tracking of fuel cells," *Applied Mathematical Modelling*, vol. 45, pp. 1067–1075, 2017.

[5] S. Ahmadi, S. Abdi, and M. Kakavand, "Maximum power point tracking of a proton exchange membrane fuel cell system using pso-pid controller," *International journal of hydrogen energy*, vol. 42, no. 32, pp. 20430–20443, 2017.

[6] E. Akbari, A. R. Sheikholeslami, and F. Zishan, "Participation of renewable energy in providing demand response in presence of energy storage," *Renewable Energy Research and Applications*, vol. 4, no. 2, pp. 225–234, 2023.

[7] F. Gao, M. Kabalo, M. S. Rylko, B. Blunier, and A. Miraoui, "Fuel cell system," *Power Electronics for Renewable and Distributed Energy Systems: A Sourcebook of Topologies, Control and Integration*, pp. 185–234, 2013.

[8] N. Naseri, S. El Hani, A. Aghmadi, K. El Harouri, M. S. Heyine, and H. Mediouni, "Proton exchange membrane fuel cell modelling and power control by p&o algorithm," in *2018 6th International Renewable and Sustainable Energy Conference (IRSEC)*, pp. 1–5, IEEE, 2018.

[9] M. H. Wang, M.-L. Huang, W.-J. Jiang, and K.-J. Liou, "Maximum power point tracking control method for proton exchange membrane fuel cell," *IET Renewable Power Generation*, vol. 10, no. 7, pp. 908–915, 2016.

[10] N. Karami, L. El Khoury, G. Khoury, and N. Moubayed, "Comparative study between p&o and incremental conductance for fuel cell mppt," in *International conference on renewable energies for developing countries 2014*, pp. 17–22, IEEE, 2014.

[11] D. N. Luta and A. K. Raji, "Fuzzy rule-based and particle swarm optimisation mppt techniques for a fuel cell stack," *Energies*, vol. 12, no. 5, p. 936, 2019.

[12] J. Jiao and X. Cui, "Adaptive control of mppt for fuel cell power system," *J. Converg. Inf. Technol*, vol. 8, no. 4, pp. 362–371, 2013.

[13] K. Afshar, N. Bigdeli, and S. Ahmadi, "A novel approach for robust maximum power point tracking of pem fuel cell generator using sliding mode control approach," *International Journal of Electrochemical Science*, vol. 7, no. 5, pp. 4192–4209, 2012.

[14] M. Derbeli, O. Barambones, M. Y. Silaa, and C. Napole, "Real-time implementation of a new mppt control method for a dc-dc boost converter used in a pem fuel cell power system," in *Actuators*, vol. 9, p. 105, MDPI, 2020.

[15] J. C. Amphlett, R. Baumert, R. F. Mann, B. A. Peppley, P. R. Roberge, and T. J. Harris, "Performance modeling of the ballard mark iv solid polymer electrolyte fuel cell: Ii. empirical model development," *Journal of the Electrochemical Society*, vol. 142, no. 1, p. 9, 1995.

[16] J. M. Correa, F. A. Farret, and L. N. Canha, "An analysis of the dynamic performance of proton exchange membrane fuel cells using an electrochemical model," in *IECON'01. 27th Annual Conference of the IEEE Industrial Electronics Society (Cat. No. 37243)*, vol. 1, pp. 141–146, IEEE, 2001.

[17] Y. Chen and N. Wang, "Cuckoo search algorithm with explosion operator for modeling proton exchange membrane fuel cells," *International Journal of Hydrogen Energy*, vol. 44, no. 5, pp. 3075–3087, 2019.

[18] M. Derbeli, O. Barambones, M. Farhat, and L. Sbita, "Efficiency boosting for proton exchange membrane fuel cell power system using new mppt method," in *2019 10th International Renewable Energy Congress (IREC)*, pp. 1–4, IEEE, 2019.

[19] R. Abdul-Halem, H. A. Hairik, and A. J. Kadhem, "Experimental prototype for pwm-based sliding mode boost converter," in *2010 1st International Conference on Energy, Power and Control (EPC-IQ)*, pp. 230–236, IEEE, 2010.

[20] S. Mirjalili, S. M. Mirjalili, and A. Lewis, "Grey wolf optimizer adv eng softw 69: 46–61," *ed*, 2014.

[21] F. Liu, Y. Kang, Y. Zhang, and S. Duan, "Comparison of p&o and hill climbing mppt methods for grid-connected pv converter," in *2008 3rd IEEE Conference on Industrial Electronics and Applications*, pp. 804–807, IEEE, 2008.

[22] M. A. G. De Brito, L. Galotto, L. P. Sampaio, G. d. A. e Melo, and C. A. Canesin, "Evaluation of the main mppt techniques for photovoltaic applications," *IEEE transactions on industrial electronics*, vol. 60, no. 3, pp. 1156–1167, 2012.